European Journal of Chemistry

View Journal Online
View Article Online

Bivalent metal complexes of a novel modified nicotinic acid hydrazide drug: Synthesis, characterization, and anti-tubercular studies

Cyprian Chunkang Mikwa [1], Gwendoline Mochia Toh-Boyo [1], Romanus Nyako Njong [2], Bridget Ndosiri Ndoye [3], Christophe Adrien Ndamyabera [4], Natsuki Katsuumi [5], Yuta Mitani [5], Emmanuel Ngwang Nfor [1,*] and Takashiro Akitsu [5]

[1] *Department of Chemistry, Faculty of Science, University of Buea, Buea, PO Box 63, Cameroon*
[2] *Department of Fundamental Sciences, Higher Technical Teacher Training College, The University of Bamenda, Bambili, PO Box 39, Cameroon*
[3] *Department of Inorganic Chemistry, Faculty of Science, University of Yaoundé 1, Yaoundé, PO Box 812, Cameroon*
[4] *Department of Chemistry, Centre for Supramolecular Chemistry Research, University of Cape Town, Rondebosch 7701, South Africa*
[5] *Department of Chemistry, Faculty of Science, Tokyo University of Science, 1-3 Kagurazaka, Shinjuku-Ku, Tokyo 162-8601, Japan*

* *Corresponding author at: Department of Chemistry, Faculty of Science, University of Buea, Buea, PO Box 63, Cameroon.*
e-mail: nfor.emmanuel@ubuea.cm (E.N. Nfor).

RESEARCH ARTICLE

10.5155/eurjchem.13.1.63-68.2183

Received: 08 September 2021
Received in revised form: 18 November 2021
Accepted: 20 November 2021
Published online: 31 March 2022
Printed: 31 March 2022

KEYWORDS

Schiff base
Complexes
Hydrazones
Crystal structure
Anti-tubercular activity
Nicotinic acid hydrazide

ABSTRACT

Iron(II) and manganese(II) complexes of *N*'-(1-(pyridin-2-yl)ethylidene)nicotinohydrazide (LH) have been synthesized and characterized by elemental analysis, IR, and ^{1}H NMR spectroscopy. The crystal structure of the ligand has been determined by single crystal X-ray diffraction and electronic spectroscopic techniques. Crystal data for LH, $C_{13}H_{12}N_4O$: Orthorhombic, space group *Pbcn* (no. 60), a = 18.0824(3) Å, b = 7.86555(14) Å, c = 16.1614(3) Å, V = 2298.60(7) Å^3, Z = 8, T = 103 K, μ(Mo Kα) = 0.093 mm^{-1}, *Dcalc* = 1.388 g/cm^3, 36729 reflections measured (5.042° ≤ 2Θ ≤ 54.966°), 2633 unique (R_{int} = 0.0224, R_{sigma} = 0.0124) which were used in all calculations. The final R_1 was 0.0383 ($F^2>2\sigma(F^2)$) and wR_2 was 0.0988 (all data). The ligand was found to chelate to the metal ions through the azomethine nitrogen and amide oxygen atoms in a bidentate manner. The anti-tubercular activity of the ligand, its iron (II) and manganese (II) complexes were studied against *Mycobacterium tuberculosis* (ATTC 27294). The results revealed higher activity of the iron (II) complex with MIC value of 8.00±0.83 μM and a moderate activity of the manganese (II) complex having MIC value of 14.20±1.40 μM, compared to the reference drugs having MIC values of 9.41±0.92, 10.74±1.02, 25.34±2.6 μM and parent ligand with MIC value of 17.60±1.80 μM.

Cite this: *Eur. J. Chem.* **2022**, *13(1)*, 63-68 **Journal website**: www.eurjchem.com

1. Introduction

Nicotinic acid hydrazide, which was first introduced in tuberculosis therapy in the 1950 [1], is regarded as one of the most commonly used and efficient drugs in the treatment of human tuberculosis [2]. Over one-third of the global population is said to be infected by tuberculosis leading to an approximate death rate of two to three million people annually [3]. There have been reports of increased incidence of multidrug resistance and extensively drug resistant strains of *mycobacterium tuberculosis* which compromises the recurrent effective treatment, prompting the need for the search of novel anti-tuberculosis agents [4-6]. The modification of existing drugs and the development of novel active compounds by synthetic medicinal chemists have been contributing to the strategies adopted to improve tuberculosis therapy [7-9]. In this regards, nicotinic acid hydrazide is one of the most researched anti-tubercular agents as evident in several reports of a range of its analogues, with anti-tubercular potentials and a number of promising candidates [10,11-15]. Inspired by these considerations, and in continuation with our studies on hydrazone Schiff bases derived from similar acid hydrazides [15,16-18], we herein report on the synthesis and characterization of iron (II) and manganese (II) complexes of a Schiff base for anti-tubercular activities.

2. Experimental

2.1. Materials and physical measurements

Elemental analysis was performed on a Thermo Flash EA-1112 Series CHNS-O Elemental Analyzer. The IR spectra were obtained from KBr pellets in the range 4000-400 cm^{-1}, using a Perkin-Elmer Spectrum 100 FT-IR spectrometer. UV-Vis spectra were recorded at room temperature on a Cintra 5GBC spectrophotometer in ethanol. ^{1}H NMR spectra were recorded on a Varian Unity plus 400 MHz instrument.

https://dx.doi.org/10.5155/eurjchem.13.1.63-68.2183

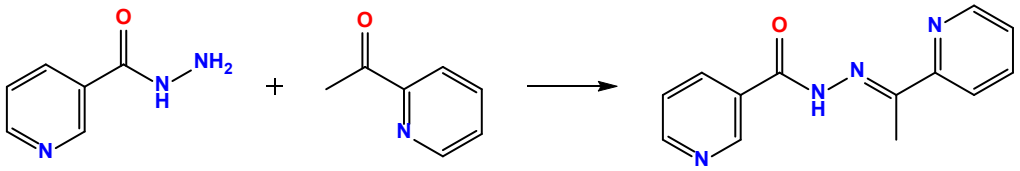

Scheme 1. Synthesis of *N*'-(1-(pyridin-2-yl)ethylidene)nicotinohydrazide.

2.2. Single crystal X-ray diffraction analysis and structure determination

A colorless block crystal of $C_{13}H_{12}N_4O$ having approximated dimensions of 0.120×0.110×0.100 mm was mounted on a glass fiber. All measurements were made at 203 K on a Rigaku R-AXIS RAPID diffractometer using multi-layer mirror monochromated MoKα radiation (λ = 0.071069 nm). The structure was solved by direct methods [19] and expanded using Fourier techniques. The non-hydrogen atoms were refined anisotropically. Hydrogen atoms were refined using the riding model. The final cycle of full-matrix least-squares refinement [20] on F^2 was based on 2633 observed reflections and converged (The largest parameter shift was 0.00 times its e.s.d.) with an un weighted and weighted agreement factor. All calculations were performed using the crystal structure crystallographic software package [21] except for refinement, which was performed using SHELXL Version 2018/3 [19].

2.3. Anti-tuberculosis evaluation

The antimicrobial activities of the new hydrazone ligand (**LH**), its iron (II), and manganese (II) complexes against *M. tuberculosis* (ATTC 27294) were evaluated by the method reported by Maria and Lourenco [22]. The reference drugs used to evaluate the potency of the synthesized compounds were ciprofloxain (MIC = 9.41±0.92 µM), pyrazinamide (MIC = 25.34±2.6 µM) and streptomycin (MIC = 10.74±1.02 µM).

2.4. Synthesis of N'-(1-(pyridin-2-yl)ethylidene)nicotine hydrazide

2-Acetylpyridine (1.620 g, 0.01 mmol) was added to nicotinic acid hydrazide (1.837 g, 0.01 mmol) in 25 mL of ethanolic solution with three drops of glacial acetic acid added as catalyst. The resulting mixture was refluxed for five hours at a temperature of 80 °C with continuous stirring. The product was left to cool overnight, removed by vacuum filtration; the precipitate was washed several times with water, ethanol, and diethyl ether and dried in a desiccator. Yellow crystals suitable for single crystal X-ray diffraction studies were obtained from the ethanolic filtrate after 30 days (Scheme 1).

N'-(1-(pyridin-2-yl)ethylidene)nicotinohydrazide: Color: Yellow. Yield: 80%. M.p.: 205-207 °C. FT-IR (KBr, ν, cm^{-1}): 3600 (OH), 3200 (N-H), 1700 (C=O), 1583 (C=N), 900-781 (C-H, Ar). ^{1}H-NMR (400 MHz, DMSO-d_6, δ, ppm): 1.62 (s, 3H, CH_3), 7.28 (m, 1H, Ar-H), 7.43 (m, 1H, Ar-H),7.66 (sbr, 1H, Ar-H), 7.83 (sbr, 1H, Ar-H), 8.23 (d, *J* = 10.4 Hz, 1H, Ar-H), 8.57 (d, *J* = 6.0 Hz, 1H, Ar-H), 8.76 (sbr, 1H, Ar-H), 8.99 (sbr, 1H, Ar-H), 9.19 (sbr, 1H, N-H). MS (EI, *m/z* (%)): 240.10 (M^+, 100). HRMS (EI, *m/z*) calcd. for $C_{13}H_{12}N_4O$, 240.10; Found: 241.10. UV/Vis ($CHCl_3$, λ_{max}, nm, (ε)): 230 (3.42), 280 (3.62), 330 (4.62), 308 (4.48), 391 (5.32). Anal. calcd. for $C_{13}H_{12}N_4O$: C, 64.99; H, 5.03; N, 23.32. Found: C, 64.97; H, 4.96; N, 23.37%.

2.5. Synthesis of manganese (II) complex

Manganese (II) chloride tetrahydrate (0.199 g, 1.0 mmol) was added to *N*'-(1-(pyridin-2-yl)ethylidene)nicotinohydrazide (0.480 g, 2.0 mmol) in a 25 mL ethanolic solution. The resulting mixture was refluxed for 5 hours at a temperature of 90 °C with continuous stirring using a magnetic stirrer. The pale-yellow solution obtained was allowed to cool overnight, the precipitate removed by filtration; washed with ethanol and stored in a desiccator. *Manganese (II) complex*: Color: Yellowish. Yield: 85%. FT-IR (KBr, ν, cm^{-1}): 3600 (OH), 2990 (N-H), 1620 (C=O), 1470 (C=N), 600-750 (C-H), 580 (Mn-O), 470 (Mn-N). ^{1}H NMR (400 MHz, DMSO-d_6, δ, ppm): 2.08 (s, 6H, CH_3), 6.86 (m, 3H, Ar-H), 6.99 (s, *J* = 8 Hz, 2H, Ar-H), 7.12 (d, *J* = 8 Hz, 2H, Ar-H), 7.53 (t, *J* = 8 Hz, 2H, Ar-H), 7.61 (sbr, 3H, Ar-H), 7.90 (d, *J* = 8 Hz, 1H, Ar-H), 8.25 (s, 1H, Ar-H), 10.81 (d, 2H, Ar-H), 11.97 (s, 2H, N-H). Anal. calcd. for $C_{26}H_{24}Cl_2MnN_8O_2$: C, 51.50; H, 3.99; N, 18.48. Found: C, 51.97; H, 3.90; N, 18.37%.

2.6. Synthesis of iron (II) complex

Iron (II) chloride tetrahydrate (0.198 g, 1.0 mmol) was added to *N*'-(1-(pyridin-2-yl)ethylidene)nicotinohydrazide (0.480 g, 2.0 mmol) in a 25 mL ethanolic solution. The resulting mixture was refluxed for 5 hours at a temperature of 80 °C with continuous stirring using a magnetic stirrer. The reddish-brown solution obtained was allowed to cool overnight; the precipitate was removed by filtration, washed with ethanol and stored in a desiccator. *Iron (II) complex*: Color: Brownish. Yield: 85%. FT-IR (KBr, ν, cm^{-1}): 3600 (OH), 2980 (N-H), 1650 (C=O), 1525 (C=N), 750-800 (C-H), 530 (Fe-O), 460 (Fe-N). ^{1}H NMR (400 MHz, DMSO-d_6, δ, ppm): 2.08 (s, 6H, CH_3), 6.97 (m, 3H, Ar-H), 6.99 (s, *J* = 8 Hz, 2H, Ar-H), 7.13 (d, *J* = 8 Hz, 2H, Ar-H), 7.40 (t, *J* = 8 Hz, 2H, Ar-H), 7.44 (sbr, 3H, Ar-H), 7.60 (d, *J* = 8 Hz, 1H, Ar-H), 8.29 (s, 1H, Ar-H), 8.31 (d, 2H, Ar-H), 11.38 (s, 2H, N-H). Anal. calcd. for $C_{26}H_{24}Cl_2FeN_8O_2$: C, 51.42; H, 3.98; N, 18.45. Found: C, 51.60; H, 3.98; N, 18.30%.

3. Results and discussion

3.1. Synthesis

The elemental analysis for C, H, and N revealed that the calculated and experimental data for the Schiff base ligand **LH** are in agreement, thus confirming the proposed molecular formula $C_{13}H_{12}N_4O$ for the ligand. The agreement between the calculated and experimental elemental analyses values for the metal complexes revealed a 1:2 (metal-ligand) stoichiometry, thus confirming their suggested formulae. These results further confirm the high purity of the prepared compounds.

The infrared spectra of the ligand **LH** and its metal (II) complexes were recorded within the 4000-400 cm^{-1} region. The IR-spectrum of the hydrazone ligand exhibited a medium band at 3600 cm^{-1} and a broad band at 3200 cm^{-1} attributed to ν(OH) of the coordinated water molecule and ν(NH) stretching vibrations, respectively. The strong bands at 1700 and 1583 cm^{-1} in the spectrum of the ligand, corresponds to the presence of ν(C=O) [23] and ν(C=N) vibration modes [16]. Bands appearing at 995, 939, 800, and 781 cm^{-1} in the spectrum of **LH** are the usual modes of C-H of the aromatic ring vibrations and these revealed small shifts in the metal (II) complexes compared to the free ligand, which is the expected electronic structure changes that occur with coordination of the ligand to metal (II) ions.

Table 1. Crystal data and structure refinement of *N*'-(1-(pyridin-2-yl)ethylidene)nicotinohydrazide.

Empirical formula	$C_{13}H_{12}N_4O$
Formula weight	240.26
Temperature (K)	103
Crystal system	Orthorhombic
Space group	*Pbcn*
a, (Å)	18.0824(3)
b, (Å)	7.86555(14)
c, (Å)	16.1614(3)
Volume (Å^3)	2298.60(7)
Z	8
ρ_{calc}(g/cm^3)	1.388
μ (mm^{-1})	0.093
F(000)	1008
Crystal size (mm^3)	0.12 × 0.11 × 0.1
Radiation	Mo Kα (λ = 0.71075)
2Θ range for data collection (°)	5.042 to 54.966
Index ranges	-23 ≤ *h* ≤ 23, -10 ≤ *k* ≤ 10, -20 ≤ *l* ≤ 20
Reflections collected	36729
Independent reflections	2633 [R_{int} = 0.0224, R_{sigma} = 0.0124]
Data/restraints/parameters	2633/0/164
Goodness-of-fit on F^2	1.049
Final R indexes [I≥2σ (I)]	R_1 = 0.0383, wR_2 = 0.0974
Final R indexes [all data]	R_1 = 0.0402, wR_2 = 0.0988
Largest diff. peak/hole (e.Å^{-3})	0.44/-0.27

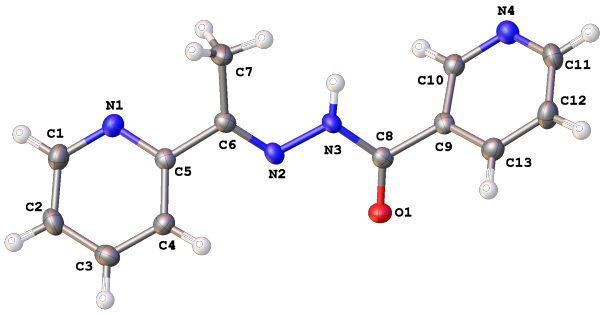

Figure 1. Molecular structure of **LH** with atom numbering scheme.

In the spectrum of the manganese (II) complex, the *ν*(C=O) and *ν*(C=N) vibration bands experience negative shifts to 1620 cm^{-1} and 1470 cm^{-1}, respectively, compared to the ligand. This indicates the coordination the carbonyl oxygen and the azomethine nitrogen atoms to the manganese (II) ion. In the low frequency region, the bands in the region 580 and 470 cm^{-1} are probably due to *ν*(Mn-O) and *ν*(Mn-N) vibrations, respectively. In the spectrum of the iron (II) complex, the *ν*(C=O) and *ν*(C=N) vibration bands have also experienced a negative shift to the frequencies of 1650 and 1525 cm^{-1}, respectively, indicating coordination of the carbonyl oxygen and the azomethine nitrogen atoms to the iron (II) ion. In the low frequency region, the bands in the regions 460 and 530 cm^{-1} are probably due to the *ν*(Fe-O) and *ν*(Fe-N) vibrations, respectively [24-26]. In both complexes, the broad bands at 3600 and 2980 cm^{-1} are attributed to *ν*(OH) of the coordinated water molecule and *ν*(NH) of the amide.

The structural features of the ligand and its metal (II) complexes in this investigation are supported by the ^{1}H NMR spectra obtained in DMSO-d_6 solution. In the ^{1}H NMR spectrum of the ligand, the multiplets at δ 7.28-8.99 ppm are attributed to the pyridyl rings protons. The amide proton is attributed to the signals at δ 9.19 ppm in the ligand. The methyl protons in this ligand are visible at δ 1.62 ppm. In the manganese complex, the pyridyl ring protons are attributed to the signals at δ 6.86-10.81 ppm, with the amide proton attributed to the signal at δ 11.97 ppm. The methyl proton in this complex is attributed to the signal at δ 2.08 ppm. The iron complex also exhibited signals at between δ 6.97-8.31 ppm attributed to the pyridyl ring protons, while the amide proton further exhibited signal at δ 11.38 ppm. The methyl proton signal in this complex is visible at δ 2.08 ppm. All the changes in the signals of the pyridyl ring, amide and methyl protons in the metal (II) complexes, suggests the involvement of the azomethine nitrogen and carbonyl oxygen atoms in coordination [16,27]. In the UV spectrum of **LH**, two relatively intense peaks were observed at 230 and 280 nm, attributed to the n-π* of the aromatic rings and the others peaks attributed to the azomethine group transitions are observed at 308-315 nm [28].

3.2. Crystal structure analysis

The molecular structure of *N*'-(1-(pyridin-2-yl)ethylidene) nicotinohydrazide is shown in Figure 1 along with the atomic numbering scheme. The crystal structure refinement data for **LH** is shown in Table 1. The bond lengths, bond angles, and torsion angles of **LH** are listed in Table 2. The Schiff base **LH** crystallizes in the orthorhombic system in the space group *Pcbn*. In **LH**, the bond distance C(6)-N(2) is equal to 1.2781(2) Å indicating its double bond nature. The bond lengths N(1)-C(1), N(1)-C(5), N(4)-C(10), and N(4)-C(11) are equal to 1.3427(14), 1.3472(13), 1.3408(13), and 1.3388(14), respectively. These data are indicated that this molecule has the endocyclic double bonds. The bond distance C(11)-O(18) is equal to 1.2282(2) Å, corresponding to the double bond length reported in similar Schiff bases [29,30]. Hydrogen bond interactions are listed in Table 3. The packing of the molecules when viewed along the *a*-axis is shown in Figure 2.

3.3. Anti-tuberculosis activity

The evaluation of the antitubercular activities of the ligand, its iron (II) and manganese (II) complexes against *Mycobacterium tuberculosis* was carried out using streptomycin, Ciprof-

Table 2. The bond lengths, bond angles, and torsion angles of *N*'-(1-(pyridin-2-yl)ethylidene)nicotinohydrazide.

Atom	Atom		Length (Å)	Atom	Atom		Length (Å)
O1	C8		1.2282(13)	C3	C4		1.3846(15)
N1	C1		1.3427(14)	C4	C5		1.3946(14)
N1	C5		1.3472(13)	C5	C6		1.4908(14)
N2	N3		1.3783(12)	C6	C7		1.5002(14)
N2	C6		1.2871(13)	C8	C9		1.4966(14)
N3	C8		1.3608(13)	C9	C10		1.3922(14)
N4	C10		1.3408(13)	C9	C13		1.3919(14)
N4	C11		1.3388(14)	C11	C12		1.3910(15)
C1	C2		1.3878(16)	C12	C13		1.3879(15)
C2	C3		1.3915(15)				
Atom	**Atom**	**Atom**	**Angle (°)**	**Atom**	**Atom**	**Atom**	**Angle (°)**
C1	N1	C5	117.47(9)	N2	C6	C7	127.93(10)
C6	N2	N3	118.60(9)	C5	C6	C7	118.09(9)
C8	N3	N2	116.90(8)	O1	C8	N3	124.04(9)
C11	N4	C10	116.78(9)	O1	C8	C9	121.81(9)
N1	C1	C2	123.43(10)	N3	C8	C9	114.14(9)
C1	C2	C3	118.60(10)	C10	C9	C8	122.07(9)
C4	C3	C2	118.74(10)	C13	C9	C8	119.17(9)
C3	C4	C5	118.98(9)	C13	C9	C10	118.75(9)
N1	C5	C4	122.76(9)	N4	C10	C9	123.53(9)
N1	C5	C6	115.75(9)	N4	C11	C12	123.93(10)
C4	C5	C6	121.49(9)	C13	C12	C11	118.57(10)
N2	C6	C5	113.93(9)	C12	C13	C9	118.30(10)
A	**B**	**C**	**D** **Angle (°)**	**A**	**B**	**C**	**D** **Angle (°)**
O1	C8	C9	C10 126.73(11)	C2	C3	C4	C5 0.34(15)
O1	C8	C9	C13 -54.36(14)	C3	C4	C5	N1 1.10(15)
N1	C1	C2	C3 -0.04(17)	C3	C4	C5	C6 -178.88(9)
N1	C5	C6	N2 -147.36(9)	C4	C5	C6	N2 32.62(13)
N1	C5	C6	C7 30.35(13)	C4	C5	C6	C7 -149.68(10)
N2	N3	C8	O1 3.17(15)	C5	N1	C1	C2 1.41(16)
N2	N3	C8	C9 -175.91(8)	C6	N2	N3	C8 178.93(9)
N3	N2	C6	C5 177.57(8)	C8	C9	C10	N4 177.63(9)
N3	N2	C6	C7 0.13(16)	C8	C9	C13	C12 -175.56(9)
N3	C8	C9	C10 -54.17(13)	C10	N4	C11	C12 3.12(16)
N3	C8	C9	C13 124.75(10)	C10	C9	C13	C12 3.39(15)
N4	C11	C12	C13 -1.02(17)	C11	N4	C10	C9 -1.93(15)
C1	N1	C5	C4 -1.94(15)	C11	C12	C13	C9 -2.32(16)
C1	N1	C5	C6 178.04(9)	C13	C9	C10	N4 -1.29(16)
C1	C2	C3	C4 -0.84(16)				

Table 3. Geometry of hydrogen bond interactions for *N*'-(1-(pyridin-2-yl)ethylidene)nicotinohydrazide.

Donor-H···Acceptor	D-H (Å)	H···A (Å)	D···A (Å)	∠D-H···A (°)	Symmetry
N(3)-H(3)···O(1)	0.88	2.22	3.0887(12)	169	1/2-*x*, 1/2+*y*, *z*
N(3)-H(3)···N(2)	0.88	2.58	3.1080(12)	119'	1/2-*x*, 1/2+*y*, *z*
C(7)-H(7A)···N(3)	0.98	2.51	2.8691(14)	101	-
C(7)-H(7A)···O(1)	0.98	2.32	3.1900(14)	148'	1/2-*x*, 1/2+*y*, *z*

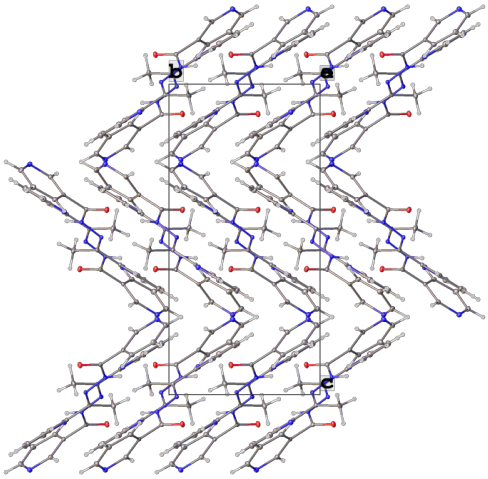

Figure 2. Packing of molecules viewed along the *a*-axis.

loxacin, and pyrazinamide as reference drugs. The iron (II) complex with MIC 8.00±0.83 µM exhibited the highest anti-tuberculosis activity compared to the manganese (II) complex with MIC value of 14.2±1.40 µM and all standards as shown in Table 4. The ligand with MIC value 17.6±1.80 µM exhibited the least activity compared to its metal complexes. This may be attributed to the reduced polarity of the central metals (II) ions which partially share their positive charges with the donor groups as well as the possible π-electron delocalization within the entire chelating ring system formed during coordination. This enhances the lipophilic character of the central metal atoms/ions, thereby increasing their hydrophobic character and favoring their ability to permeate the lipid layers of the cell membrane as explained by the Tweedy's chelation theory [31].

Table 4. Anti-tubercular activity of ligand and its metal (II) complexes *.

Test sample	Sample concentration in µM (MIC)±SD
Ligand (LH)	17.60±1.80
$Fe(LH)_2Cl_2$	8.00±0.83
$Mn(LH)_2Cl_2$	14.20±1.40
Ciprofloxacin	9.41±0.92
Streptomycin	10.74±1.02
Pyrazinamide	25.34±2.60

* Values expressed are mean±SD of three parallel measurements.

Overall, the results showed higher activity of the metal (II) complexes against *M. tuberculosis* as compared to the standard drug pyrazinamide, and a moderate activity as compared to streptomycin and ciprofloxacin drugs.

4. Conclusion

We have synthesized iron (II) and manganese (II) complexes of nicotinic acid hydrazide derived Schiff base compound. The prepared compounds were characterized using FT-IR, ^{1}H NMR spectroscopy, XRD, and UV-vis spectroscopic techniques and investigated for anti-tuberculosis activities. The prepared ligand chelates to the metal center in a bidentate manner through the azomethine nitrogen and the amide oxygen atoms to form an octahedral geometry of the metal (II) complexes. The iron (II) complex exhibited a higher activity while the manganese (II) complex showed a moderate activity against *Mycobacterium tuberculosis* compared to the reference drugs and parent ligand.

Acknowledgements

This work was supported (in part) by Nanotechnology Platform of Ministry of Education, Culture, Sports, Science and Technology (MEXT), Japan, Number JPMXP09S20NR0016 and by a Grant-in-Aid for Scientific Research (KAKENHI) number 20H00336. The authors thank Shohei Katao, Nara Institute of Science and Technology (NAIST), Japan, for X-ray crystallography. The authors are grateful to Professor Susan A. Bourne of Cape Town University in South Africa for the spectral analysis.

Supporting information

CCDC-2090758 contains the supplementary crystallographic data for *N*'-(1-(pyridin-2-yl)ethylidene)nicotinohydrazide. These data can be obtained free of charge via http://www.ccdc.cam.ac.uk/conts/retrieving.html, or by e-mailing data_request@ccdc.cam.ac.uk, or by contacting The Cambridge Crystallographic Data Centre, 12 Union Road, Cambridge CB2 1EZ, UK; fax: +44(0)1223-336033.

Disclosure statement

Conflict of interests: The authors declare that they have no conflict of interest.
Ethical approval: All ethical guidelines have been adhered.
Sample availability: Samples of the compounds are available from the author.

CRediT authorship contribution statement

Conceptualization: Emmanuel Ngwang Nfor, Takashiro Akitsu; Methodology: Cyprian Chunkang Mikwa, Gwendoline Mochia Toh-Boyo; Software: Yuta Mitani, Natsuki Katsuumi; Formal Analysis: Christophe Adrien Ndamyabera; Writing - Original Draft: Bridget Ndosiri Ndoye, Romanus Nyako Njong; Writing - Review and Editing: Emmanuel Ngwang Nfor, Takashiro Akitsu; Funding acquisition: Takashiro Akitsu.

ORCID and Email

Cyprian Chunkang Mikwa
mchunkang@yahoo.com
https://orcid.org/0000-0003-4101-0195
Gwendoline Mochia Toh-Boyo
gwendoline.mochia@ubuea.cm
https://orcid.org/0000-0002-9785-6678
Romanus Nyako Njong
njong74@gmail.com
https://orcid.org/0000-0001-7429-6332
Bridget Ndosiri Ndoye
ndosirin@yahoo.com
https://orcid.org/0000-0001-7969-8963
Christophe Adrien Ndamyabera
ndmchr002@myuct.ac.za
https://orcid.org/0000-0002-2605-319X
Natsuki Katsuumi
1320529@ed.tus.ac.jp
https://orcid.org/0000-0002-0423-4360
Yuta Mitani
1320605@ed.tus.ac.jp
https://orcid.org/0000-0001-8082-4293
Emmanuel Ngwang Nfor
nfor.emmanuel@ubuea.cm
https://orcid.org/0000-0002-0868-8917
Takashiro Akitsu
akitsu2@rs.tus.ac.jp
https://orcid.org/0000-0003-4410-4912

References

[1]. Judge, V.; Narasimhan, B.; Ahuja, M. Isoniazid: The Magic Molecule. *Med. Chem. Res.* **2012**, *21* (12), 3940–3957.
[2]. van den Boogaard, J.; Kibiki, G. S.; Kisanga, E. R.; Boeree, M. J.; Aarnoutse, R. E. New Drugs against Tuberculosis: Problems, Progress, and Evaluation of Agents in Clinical Development. *Antimicrob. Agents Chemother.* **2009**, *53* (3), 849–862.
[3]. World Health Organization, Global Tuberculosis Report, 2017. https://www.who.int/tb/publications/global_report/gtbr2017 (accessed Nov 19, 2021).
[4]. Prozorov, A. A.; Zaichikova, M. V.; Danilenko, V. N. Mycobacterium Tuberculosis Mutants with Multidrug Resistance: History of Origin, Genetic and Molecular Mechanisms of Resistance, and Emerging Challenges. *Russ. J. Genet.* **2012**, *48* (1), 1–14.
[5]. Sotgiu, G.; Ferrara, G.; Matteelli, A.; Richardson, M. D.; Centis, R.; Ruesch-Gerdes, S.; Toungoussova, O.; Zellweger, J.-P.; Spanevello, A.; Cirillo, D.; Lange, C.; Migliori, G. B. Epidemiology and Clinical Management of XDR-TB: A Systematic Review by TBNET. *Eur. Respir. J.* **2009**, *33* (4), 871–881.
[6]. Hoagland, D. T.; Liu, J.; Lee, R. B.; Lee, R. E. New Agents for the Treatment of Drug-Resistant Mycobacterium Tuberculosis. *Adv. Drug Deliv. Rev.* **2016**, *102*, 55–72.
[7]. Wong, E. B.; Cohen, K. A.; Bishai, W. R. Rising to the Challenge: New Therapies for Tuberculosis. *Trends Microbiol.* **2013**, *21* (9), 493–501.
[8]. Ellis, S.; Kalinowski, D. S.; Leotta, L.; Huang, M. L. H.; Jelfs, P.; Sintchenko, V.; Richardson, D. R.; Triccas, J. A. Potent Antimycobacterial Activity of the Pyridoxal Isonicotinoyl Hydrazone Analog 2-Pyridylcarboxaldehyde Isonicotinoyl Hydrazone: A Lipophilic Transport Vehicle for Isonicotinic Acid Hydrazide. *Mol. Pharmacol.* **2014**, *85* (2), 269–278.
[9]. Chaves, J. D. S.; Damasceno, J. L.; Paula, M. C. F.; de Oliveira, P. F.; Azevedo, G. C.; Matos, R. C.; Lourenço, M. C. S.; Tavares, D. C.; Silva, H.; Fontes, A. P. S.; de Almeida, M. V. Synthesis, Characterization, Cytotoxic and Antitubercular Activities of New Gold(I) and Gold(III) Complexes Containing Ligands Derived from Carbohydrates. *Biometals* **2015**, *28* (5), 845–860.
[10]. Oludina, Y. N.; Voloshina, A. D.; Kulik, M. V.; Zobov, V. V.; Bukharov, S. V.; Tagasheva, R. G.; Nugumanova, G. N.; Burilov, A. R.; Kravchenko, M. A.; Skornyakov, S. N.; Rusinov, G. L. Synthesis, Toxicity, and Antituberculosis Activity of Isoniazid Derivatives Containing Sterically Hindered Phenols. *Pharm. Chem. J.* **2014**, *48* (1), 5–7.
[11]. Parumasivam, T.; Naveen Kumar, H. S.; Ibrahim, P.; Sadikun, A.; Mohamad, S. Anti-Tuberculosis Activity of Lipophilic Isoniazid Derivatives and Their Interactions with First-Line Anti-Tuberculosis Drugs. *J. Pharm. Res.* **2013**, *7* (4), 313–317.

[12]. Matei, L.; Bleotu, C.; Baciu, I.; Draghici, C.; Ionita, P.; Paun, A.; Chifiriuc, M. C.; Sbarcea, A.; Zarafu, I. Synthesis and Bioevaluation of Some New Isoniazid Derivatives. *Bioorg. Med. Chem.* **2013**, *21* (17), 5355–5361.
[13]. Ramani, A. V.; Monika, A.; Indira, V. L.; Karyavardhi, G.; Venkatesh, J.; Jeankumar, V. U.; Manjashetty, T. H.; Yogeeswari, P.; Sriram, D. Synthesis of Highly Potent Novel Anti-Tubercular Isoniazid Analogues with Preliminary Pharmacokinetic Evaluation. *Bioorg. Med. Chem. Lett.* **2012**, *22* (8), 2764–2767.
[14]. Naveen Kumar, H. S.; Parumasivam, T.; Jumaat, F.; Ibrahim, P.; Asmawi, M. Z.; Sadikun, A. Synthesis and Evaluation of Isonicotinoyl Hydrazone Derivatives as Antimycobacterial and Anticancer Agents. *Med. Chem. Res.* **2014**, *23* (1), 269–279.
[15]. Toh-Boyo, G. M.; Njong, R. N.; Babette, E. M.; Nfor, E. N. Synthesis, Spectroscopic, Molecular Modeling and Anti-Fungal Studies of Some Divalent Metal Complexes of 4-Hydroxyacetophenone Isonicotinoyl Hydrazone. *Open J. Inorg. Chem.* **2021**, *11* (03), 95–109.
[16]. Nfor, E. N.; Husian, A.; Majoumo-Mbe, F.; Njah, I. N.; Offiong, O. E.; Bourne, S. A. Synthesis, Crystal Structure and Antifungal Activity of a Ni(II) Complex of a New Hydrazone Derived from Antihypertensive Drug Hydralazine Hydrochloride. *Polyhedron* **2013**, *63*, 207–213.
[17]. Majoumo-Mbe, F.; Nfor, E. N.; Sengeh, E. B.; Njong, R. N.; Offiong, O. E. 3.3.2. Synthesis, Crystal Structure and Biological Activity of 1-(Phthalazin-1(2H)-One)[(Pyridin-2-Yl)Ethylidene]Hydrazone and Its Cobalt (III) Complex. *Commun. Inorg. Synth.* **2015**, *3* (3), 40–46. https://doi.org/10.21060/cis.v3i3.2260.
[18]. Majoumo-Mbe, F.; Nfor, N. E.; Kenfack Tsobnang, P.; Nguepmeni Eloundou, V. B.; Ngwain Yong, J.; Iris Efeti, I. Synthesis, Molecular and Crystal Structure of 1-(1,2-Dihydrophthalazin-1-Ylidene)-2-[1-(Thiophen-2-Yl)Ethylidene]Hydrazine. *Acta Crystallogr. E Crystallogr. Commun.* **2019**, *75* (2), 251–254.
[19]. Sheldrick, G. M. A Short History of SHELX. *Acta Crystallogr. A* **2008**, *64* (Pt 1), 112–122.
[20]. Sheldrick, G. M. Crystal Structure Refinement WithSHELXL. *Acta Crystallogr. C Struct. Chem.* **2015**, *71* (1), 3–8.
[21]. Rigaku. CrystalStructure. Rigaku Corporation, Tokyo, Japan, 2010.
[22]. Lourenco, M. C.; de Souza, M. V. N.; Pinheiro, A. C.; Ferreira, M. L.; Goncalves, R. S. B.; Nogneira, T. C. M.; Peralta, M. A. Evaluation of Anti-Tubercular Activity of Nicotinic and Isoniazid Analogues. *ARKIVOC* **2007**, *2007* (15), 181-191.
[23]. Pahontu, E.; Fala, V.; Gulea, A.; Poirier, D.; Tapcov, V.; Rosu, T. Synthesis and Characterization of Some New Cu(II), Ni(II) and Zn(II) Complexes with Salicylidene Thiosemicarbazones: Antibacterial, Antifungal and in Vitro Antileukemia Activity. *Molecules* **2013**, *18* (8), 8812–8836.
[24]. Muthukumar, M.; Viswanathamurthi, P. Synthesis, Spectral Characterization and Catalytic Studies of New Ruthenium(II) Chalcone Thiosemicarbazone Complexes. *Open Chem.* **2010**, *8* (1), 229–240.
[25]. Ouf, A. E.-F.; Ali, M. S.; Saad, E. M.; Mostafa, S. I. PH-Metric and Spectroscopic Properties of New 4-Hydroxysalicylidene-2-Aminopyrimidine Schiff-Base Transition Metal Complexes. *J. Mol. Struct.* **2010**, *973* (1–3), 69–75.
[26]. Nakamoto, K.; Ohkaku, N. Metal Isotope Effect on Metal-Ligand Vibrations. VI. Metal Complexes of 8-Hydroxyquinoline. *Inorg. Chem.* **1971**, *10* (4), 798–805.
[27]. Naglah, A. M.; Awad, H. M.; Bhat, M. A.; Al-Omar, M. A.; Amr, A. E.-G. E. Microwave-Assisted Synthesis and Antimicrobial Activity of Some Novel Isatin Schiff Bases Linked to Nicotinic Acid via Certain Amino Acid Bridge. *J. Chem.* **2015**, *2015*, 1–8.
[28]. Khor, Z. C.; Low, M. L.; Ling, I. Schiff Bases and Their Copper(II) Complexes Derived from Cinnamaldehyde and Different Hydrazides: Synthesis and Antibacterial Properties. *J. Transit. Met. Complexes* **2020**, *3*, 1–9.
[29]. Velezheva, V.; Brennan, P.; Ivanov, P.; Kornienko, A.; Lyubimov, S.; Kazarian, K.; Nikonenko, B.; Majorov, K.; Apt, A. Synthesis and Antituberculosis Activity of Indole-Pyridine Derived Hydrazides, Hydrazide-Hydrazones, and Thiosemicarbazones. *Bioorg. Med. Chem. Lett.* **2016**, *26* (3), 978–985.
[30]. Morjan, R. Y.; Mkadmh, A. M.; Beadham, I.; Elmanama, A. A.; Mattar, M. R.; Raftery, J.; Pritchard, R. G.; Awadallah, A. M.; Gardiner, J. M. Antibacterial Activities of Novel Nicotinic Acid Hydrazides and Their Conversion into N-Acetyl-1,3,4-Oxadiazoles. *Bioorg. Med. Chem. Lett.* **2014**, *24* (24), 5796–5800.
[31]. Nfor, E. N.; Esemu, N. S.; Ayimele, A. G.; Eno, A. E.; Iniama, E. G.; Offiong, E. O. Synthesis, Stereochemistry and Antimicrobial Activity of Copper(II) and Nickel(II) Complexes of 4-Phenylsemicarbazones. *Bull. Chem. Soc. Ethiop.* **2011**, *25* (3), 361–370.